JPL D- 57153

ECOsystem Spaceborne Thermal Radiometer Experiment on Space Station (ECOSTRESS) Mission

Level 3 Evapotranspiration Priestley-Taylor Jet Propulsion Laboratory (PT-JPL) Data User Guide

Version 2
June 18, 2019

Gregory H. Halverson
ECOSTRESS Algorithm Development Team

Joshua B. Fisher,
ECOSTRESS Science Lead

Christine M. Lee
ECOSTRESS Applications Lead

Jet Propulsion Laboratory
California Institute of Technology

Paper copies of this document may not be current and should not be relied on for official purposes. The current version is in the ECOSTRESS DocuShare Library (*) at https://bravo-lib.jpl.nasa.gov/docushare/dsweb/View/Library-509
(*) Access limited to user group

National Aeronautics and
Space Administration

JPL

Jet Propulsion Laboratory
4800 Oak Grove Drive
Pasadena, California 91109-8099
California Institute of Technology

ECOSTRESS Level 3 Evapotranspiration (PT-JPL) Data User Guide

Prepared by:

Gregory Halverson ECOSTRESS Algorithm Development Team	Date
Joshua Fisher ECOSTRESS Science Lead	Date
Christine Lee ECOSTRESS Applications Lead	Date

Approved by:

Jordan Padams ECOSTRESS Science Data System Manager	Date
Eugene Chu ECOSTRESS SDS System Engineer	Date

Concurred by:

Simon Hook ECOSTRESS Principal Investigator	Date

National Aeronautics and
Space Administration

Jet Propulsion Laboratory
4800 Oak Grove Drive
Pasadena, California 91109-8099
California Institute of Technology

*** Original signature page on file in project physical repository ***

Document Change Log

Revision	Date	Sections Changed	Author
Draft	06/13/2018	All	Laura Jewell
Draft	10/2/2018	All	Joshua Fisher, Christine Lee, Gregory Halverson
Draft	11/26/2018	References	Gregory Halverson
Version 1	12/18/2018	Document number	Gregory Halverson
Version 2	06/18/2019	Anomaly statement in introduction, corrected listing and description of daily latent heat flux	Gregory Halverson

Contacts

Readers seeking additional information about this document may contact the following ECOSTRESS Algorithm Development team members:

Gregory H. Halverson
MS 233-305J
Jet Propulsion Laboratory
4800 Oak Grove Drive
Pasadena, CA 91109
Email: gregory.h.halverson@jpl.nasa.gov
Office: (818) 393-3072

Christine M. Lee
MS 168-314
Jet Propulsion Laboratory
4800 Oak Grove Dr.
Pasadena, CA 91109
Email: Christine.M.Lee@jpl.nasa.gov
Office: (818) 354-3343

Joshua B. Fisher
MS 233-305C
Jet Propulsion Laboratory
4800 Oak Grove Dr.
Pasadena, CA 91109
Email: jbfisher@jpl.nasa.gov
Office: (818) 354-0934

1.0 TABLE OF CONTENTS

2.0 INTRODUCTION

2.1 Purpose and Scope

This document is the Data User Guide for the Level 3 data product for the ECOsystem Spaceborne Thermal Radiometer Experiment on Space Station (ECOSTRESS) project. The Level 3 (L3) PT-JPL product provides evapotranspiration (ET) produced according to the PT-JPL algorithm described in the L3 Algorithm Theoretical Basis Document (ATBD) (JPL D-94645). This document applies to the Level 3 PT-JPL product based upon data acquired by the ECOSTRESS radiometer instrument and will continued to be updated as needed. The purpose of this Data User Guide is to describe the ECOSTRESS end-user L3 data products and provide a guide for their use and interpretation.

2.2 Mission Overview

The ECOSTRESS instrument measures the temperature of plants and uses that information to better understand how much water plants use and how they respond to stress.

ECOSTRESS addresses three overarching science questions:

- How is the terrestrial biosphere responding to changes in water availability?
- How do changes in diurnal vegetation water stress impact the global carbon cycle?
- Can agricultural vulnerability be reduced through advanced monitoring of agricultural water consumptive use and improved drought estimation?

The ECOSTRESS mission answers these questions by accurately measuring the temperature of plants. Plants regulate their temperature by releasing water through pores on their leaves called stomata. If they have sufficient water, they can maintain their temperature. However, if there is insufficient water, their temperatures rise. This temperature rise can be measured with a sensor in space. ECOSTRESS uses a multispectral thermal infrared (TIR) radiometer to measure the surface temperature, deployed on the International Space Station. The instrument measures radiances at 5 spectral bands in the 8-12.5 μm range with approximately 70 by 70 meter of spatial resolution on the ground.

On September 29th 2018, ECOSTRESS experienced an anomaly with its primary mass storage unit (MSU). ECOSTRESS has a primary and secondary MSU (A and B). On December 5th, the instrument was switched to the secondary MSU and operations resumed with initial acquisitions over Australia and wider coverage resumed on January 9th 2019. The initial anomaly was attributed to exposure to high radiation regions, primarily over the Southern Atlantic Anomaly, and the acquisition strategy was revised to exclude these regions from future acquisitions. On March 14th 2019, the secondary MSU experienced an anomaly, and acquisitions are temporarily on hold. Work is underway to implement a direct streaming option, which will bypass the need for mass storage units. The streaming acquisition mode will change the format of the data being collected. Specifically, the new collection mode will eliminate the 1.6 μm (SWIR), 8.2 μm (TIR), and 9.0 μm (TIR) bands. To simplify product formats, the L1 and L2 products will continue to contain the datasets for these bands, but the datasets will contain fill values. This will be seen in products generated after May 15th 2019, when the instrument resumes operations. These changes are described in the detailed product specifications.

2.3 Applicable and Reference Documents

"Applicable" documents levy requirements on the areas addressed in this document. "Reference" documents are identified in the text of this document only to provide additional information to readers. Unless stated otherwise, the document revision level is Initial Release. Document dates are not listed, as they are redundant with the revision level.

2.3.1 Applicable Documents

ECOSTRESS Project Level 3 Science Data System Requirements (JPL D-94088).

ECOSTRESS Science Data Management Plan (JPL D-94607)

423-ICD-005 ICD Between ECOSTRESS SDS and LPDAAC

ECOSTRESS Level 1 Algorithm Theoretical Basis Documents (JPL D-94641, D-94642)

ECOSTRESS Level 1 Algorithm Specification Document

ECOSTRESS Level 2 Algorithm Theoretical Basis Documents (JPL D-94643, D-94644)

ECOSTRESS Level 2 Algorithm Specification Document

ECOSTRESS Level 3 (ET_PT-JPL) Algorithm Theoretical Basis Document (JPL D-94645)

ECOSTRESS Level 3 (ET_PT-JPL) Product Specification Document (JPL D-94636)

ECOSTRESS Level 3 (ET_PT-JPL) Algorithm Specification Document (JPL D-96970)

2.3.2 Reference Documents

2.4 ECOSTRESS Data Products

The ECOSTRESS mission will generate 13 different distributable data products (Reference Table below) . The products represent four levels of data processing, with data granules defined as an image scene. Each image scene consists of 44 scans of the instrument mirror, each scan taking approximately 1.181 seconds, and each image scene taking approximately 52 seconds. Each image scene starts at the beginning of the first target area encountered during each orbit. Each orbit is defined as the equatorial crossing of an ascending International Space Stations (ISS) orbit.

ECOSTRESS Level 0 data include spacecraft packets that have been pre-processed by the Ground Data System (GDS). Level 1 products include spacecraft engineering data, the time-tagged raw sensor pixels appended with their radiometric calibration coefficients, the black body pixels used to generate the calibration coefficients, geolocated and radiometrically calibrated at-sensor radiances of each image pixel, the geolocation tags of each pixel, and the corrected spacecraft attitude data. Level 2 products include the land surface temperature and emissivities of each spectral band retrieved from the at-sensor radiance data, and a cloud mask. Level 2 products also appear in image scene granules. Level 3 products contain evapotranspiration data derived from Level 2 data. Level 4 products contain evaporative stress index and water use efficiency derived from Level 3 data.

The ECOSTRESS products are listed in Table 1-1. This document will discuss only the Level 3 ET_PT-JPL product.

Table 1-1: ECOSTRESS Distributable Standard Products

Product type	Description
L0	Level 0 "raw" spacecraft packets
L1A_ENG	Spacecraft and instrument engineering data, including blackbody gradient coefficients
L1A_RAW_ATT	Uncorrected spacecraft ephemeris and attitude data
L1A_PIX	Raw pixel data with appended calibration coefficients
L1B_GEO	Geolocation tags, sun angles, and look angles, and calibrated, resampled at-sensor radiances
L1B_ATT	Corrected spacecraft ephemeris and attitude data
L2_LSTE	Land Surface temperature and emissivity
L2_CLOUD	Cloud mask
L3_ET_PT-JPL	Evapotranspiration retrieved from L2_LSTE using the PT-JPL Algorithm
L3_ET_ALEXI	Evapotranspiration generated using the ALEXI/DisALEXI Algorithm
L4_ESI_PT-JPL	Evaporative Stress Index generated with PT-JPL
L4_ESI_ALEXI	Evaporative Stress Index generated with ALEXI/DisALEXI
L4_WUE	Water Use efficiency
L3_L4_QA	Quality Assessment fields for all ancillary data used in L3 and L4 products

3.0 ALGORITHM AND DATA DESCRIPTION

3.1 The Level 3 role in the ECOSTRESS data system

The ECOSTRESS Level 3 process requires the Level 2 data products for surface temperature and emissivity as well as the Level 1 geolocation information, and a significant number of ancillary data products from other sources (see section 2.2.3). The L3 ET product itself is used for creating the L4 products, Evaporative Stress Index (ESI) and Water Use Efficiency (WUE).

3.2 Input data sets

3.2.1 Requirements on inputs

All input data for the L3 product must be geolocated and time-ordered, and therefore have latitude, longitude, and time associated with each pixel. We do not pose strict requirements on the input products regarding format, projection, and spatio- temporal range. Given the wide range of sources of input data (presented in section x), the fetch and reprojection pipeline described in section x is designed to take care of processing this input data into formats, projections, and subsets as required by the application code described in section x.

3.2.2 ECOSTRESS input products

ECOSTRESS input data products used for the L3 data product are:

- Level 1B – Geolocation
- Level 2 – Land surface temperature
- Level 2 – Surface emissivity
- Level 2 – Cloud Mask

3.2.3 Ancillary input products

Other ancillary input data products used for the L3 data product are:

- MODIS Land
- MODIS Atmosphere
- Landsat 8
- NCEP

See the table below for more detailed information.

Table 2-1: L3 ET (PT-JPL) Ancillary Input Products

Product	**Description**	**Provider**
MOD04_L2	MODIS/Terra Aerosol	LAADS
MOD06_L2	MODIS/Terra Cloud	LAADS
MOD07_L2	MODIS/Terra Atmospheric Profile	LAADS
L8B10	Landsat 8 Band 10 Thermal 10.6-11.19 microns	AWS
L8B11	Landsat 8 Band 11 Thermal 11.5-12.51 microns	AWS
L8B2	Landsat 8 Band 2 Blue 450-510nm	AWS
L8B3	Landsat 8 Band 3 Green 530-590nm	AWS
L8B4	Landsat 8 Band 4 Red 640-670nm	AWS
L8B5	Landsat 8 Band 5 NIR 850-880nm	AWS
L8B6	Landsat 8 Band 6 SWIR 1570-1650nm	AWS
L8BQA	Landsat 8 Quality Flags	AWS
L8MTL	Landsat 8 Metadata	AWS
air.sig995	Air Temperature at Near-Surface Sigma .995	NCEP
rhum.sig995	Relative Humidity at Near-Surface Sigma .995	NCEP
tmin.2m.gauss	Minimum Temperature at 2m	NCEP
uwnd.sig995	U-Wind at Near-Surface Sigma .995	NCEP
vwnd.sig995	V-Wind at Near-Surface Sigma .995	NCEP
MCD12Q1	Land Cover Type Yearly L3 Global 500 m SIN Grid	LP-DAAC
MCD43A2	BRDF-Albedo Quality 16-Day L3 Global 500m	LP-DAAC
MCD43A3	Albedo 16-Day L3 Global 500m	LP-DAAC
MOD13Q1	Vegetation Indices 16-Day L3 Global 250m	LP-DAAC
MOD15A2H	MODIS FPAR and LAI 8-Day L4 Global 500m	LP-DAAC
MOD44W	MODIS 250m Water Mask	LP-DAAC

Output data sets

3.2.4 Attributes of output products

The ECOSTRESS Level 3 output product fields are described in the table below:

Table 2-2: L3 ET (PT-JPL) Output fields

Field Name	Type	units	Field Data	valid min	valid max	fill
GROUP	**EVAPOTRANSPIRATION PT-JPL**					
ETinst	Float32	W/m^2	Instantaneous Evapotranspiration	0	2000	NaN
ETdaily	Float32	W/m^2	Daily Evapotranspiration	0	2000	NaN
ETcanopy	Float32	%	Canopy ET	0	100	NaN
ETsoil	Float32	%	Soil ET	0	100	NaN
ETinterception	Float32	%	ET Interceptions	0	100	NaN
ETinstUncertainty	Float32	W/m^2	ET Instantaneous Uncertainty	0	2000	NaN

All values in the L3 product are instantaneous at the time of ECOSTRESS overpass, except for daily daytime average latent heat flux (ETdaily). Instantaneous evapotranspiration (ETinst) represents instantaneous latent heat flux in watts per square meter. Uncertainty (ETinstUncertainty) represents the standard deviation of output across three models: PT-JPL, Penman Monteith, and SEBS. The PT-JPL partitions for canopy transpiration (ETcanopy), soil evaporation (ETsoil), and interception evaporation (ETinterception), are given as percentages (from zero to 100) of total latent heat flux.

4.0 SOFTWARE DESIGN

4.1 Overview

The ECOSTRESS pipeline prepares source data from a multitude of remote sensing and reanalysis data products. These source data are retrieved, preprocessed, and resampled to an ECOSTRESS scene. These preprocessed data are run through a series of models to produce the ECOSTRESS product.

4.2 Description of major code sections

4.2.1 Pre-processing pipeline

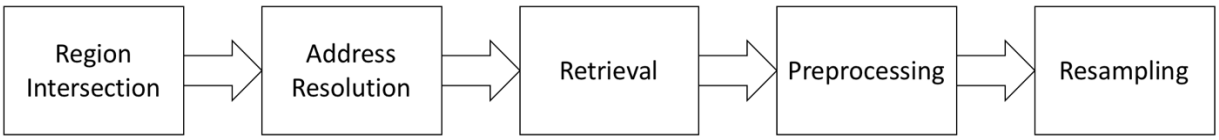

The downloader PGE begins by calculating which source data granules spatio-temporally intersect the given ECOSTRESS scene. A polygon surrounding the convex hull of latitude/longitude pairs contained in the L1B geolocation arrays is taken as the destination

region. Source regions from Landsat 8 in terms of Landsat path/row are determined by intersecting the target ECOSTRESS polygon with the static set of polygons in the WRS2-Descending region extent system. A static set of polygons in the MODIS Sinusoidal Grid are also intersected against the target footprint of the ECOSTRESS scene to select the horizontal and vertical index pairs for MODIS land products.

Selection of swath granules for the MODIS atmospheric products requires knowledge of the Terra satellite's orbit. To calculate the orbit of Terra, the Two-Line Element (TLE) observed by the Air Force at the time of ECOSTRESS overpass is queried from *spacetrack.com*. This TLE is used to calculate the swath ground track of Terra in a 12-hour radius surrounding the ECOSTRESS overpass time using the *pyephem* library. The boundary of potentially matching MODIS swath granules is calculated by dividing Terra's swath ground track into 5-minute increments beginning at UTC midnight and applying a constant cross-track swath width. The polygons surrounding these temporally intersecting MODIS swaths are then intersected against the target ECOSTRESS polygon to determine the set of MODIS swath granules that should be retrieved.

With the required granules of source data known, remote servers are crawled to resolve these granules to URLs of available granules for retrieval. Source Landsat 8 files are addressed on Amazon Web Services as individual GeoTIFF files for each band. Addresses for MODIS land data are queried from the Land Processes Distributed Active Archive Center (LP-DAAC) Inventory API. Addressed for MODIS atmosphere granules are obtained by crawling the CSV listings of the Level-1 and Atmosphere Archive & Distribution System Distributed Active Archive Center (LAADS DAAC) HTTP Interface.

With the addresses of required granules recorded, the downloader PGE makes calls to WGET to retrieve these files from the remote servers, organized into a consistent directory structure on the local filesystem. In order to conserve on storage requirements, all runs of the ECOSTRESS downloader retrieve to a collective local mirror. WGET is able to efficiently retrieve only files that it has not already retrieved.

The preprocessor PGE loads and preprocesses the retrieved source data granules. Both Landsat and MODIS record their datasets in 16-bit integer analogs to floating point values. These Digital Numbers (DNs) in the Landsat bands are converted to reflectance using linear parameters read from the Landsat metadata, and these reflectance values are used to calculate NDVI and albedo. Atmospheric and land inputs are ready-made as products in MODIS but are also linearly converted into real units and filtered by accompanying quality flags.

With source data preprocessed at their original locations, these data are ready to be projected onto the target ECOSTRESS scene. Since it is only possible to project between gridded surfaces, intermediate gridded surfaces must be created to represent the source MODIS swaths and destination ECOSTRESS swath. The *pyresample* library is used to resample by nearest neighbor between swaths and their representative grids. The *rasterio* library is used to warp data between gridded surfaces, smoothed by cubic interpolation. These techniques are combined to mosaic preprocessed source data over the extent of the ECOSTRESS scene and resample this mosaic

onto the ECOSTRESS geolocation provided by the L1B product. Finally, these data are stored as the inputs for the PT-JPL and disALEXI PGEs.

This data-store of model forcings passed to the model PGEs is organized by variable and date into a directory structure and written in Hierarchical Dataset Format (HDF5) using the *h5py* library. HDF5 was chosen as an intermediate file format to accommodate geolocated/non-gridded data.

4.2.2 Computation of evapotranspiration

The PT-JPL PGE loads the preprocessed forcing data prepared by the preprocessor PGE and runs them through a sequence of surface energy balance models. All variables, including geolocation, are loaded from the forcing data store created by the preprocessor using the HDF5 library. The Forest Light Environmental Simulator (FLiES) calculates incoming shortwave radiation from atmospheric observations. This is accomplished by querying a multidimensional array of precomputed FLiES model output as a lookup table. The Breathing Earth Systems Simulator (BESS) ingests the ECOSTRESS LST as outgoing longwave radiation. This balance is closed to produce net radiation, the total energy available at the surface. The Priestley-Taylor Jet Propulsion Laboratory (PT-JPL) model calculates transpiration, interception, and soil evaporation from net radiation using the Priestley-Taylor formula constrained by observed land surface properties. These partitions and their total are written to the ECOSTRESS product file using the HDF5 library.

5.0 OTHER CONSIDERATIONS

5.1 Error handling

Error handling is managed using Python's exception handling framework. Exception classes were designed for all foreseeable disruptions to data processing, each of which is assigned a unique exit code that is returned to the Process Control System (PCS).

5.2 Dependencies on existing software

The Anaconda distribution of Python 3.5 was chosen as the platform for the downloader/preprocessor subsystem because of its good support for geospatial data processing. The conda environment manager included in Anaconda provides seamless dependency management for the scientific, geospatial, and data management packages required for ECOSTRESS. These package dependencies include: pandas, affine, ephem, fiona, geopandas, h5py, lxml, netcdf4, nose, numpy, pyproj, python-dateutil, rasterio, requests, shapely, six, spacetrack, bs4, usgs, homura, termcolor, geocoder, scipy,

pyresample, future, pygments, xmltodict, scikit-image, jsonmerge, rasterstats, and untangle.

The C++ language was chosen to implement the PT-JPL model code to maximize the efficiency of processing large arrays. The main dependency linked to by the PT-JPL PGE is the Hierarchical Data Format (HDF) library, which is required for writing the ECOSTRESS product to file.

5.3 Assumptions and limitations

This software assumes daytime acquisition. It is designed not to run for granules acquired at night. This software also assumes precise (< 50 m) geolocation. ECOSTRESS granules that could not be precisely geolocated in the L1B GEO product are not processed into the L3 PT-JPL product. These procedures are in place to ensure that only high-quality raster data are produced in the L3 product, but results in about 1/7 of available ECOSTRESS scenes processing into PT-JPL.

This software also assumes clear-sky conditions. The cloud mask produced in the L2 LSTE product is applied to the L3 product. All pixels considered to be cloud or adjacent to clouds are represented as blank pixels by the IEEE 754 NaN value. This may result in L3 PT-JPL scenes in which a large portion or the entirety of the scene is blank.

5.4 Quality assessment and recording

No original quality flags are produced. Instead the quality flags of the source data products are resampled by nearest neighbor onto the geolocation of the ECOSTRESS scene. A quality flag array for each input dataset, when available, is collected into a combined QA product accompanying the PT-JPL product file.

6.0 APPENDIX A: ABBREVIATIONS AND ACRONYMS

ALEXI	Atmospheric-Land Exchange Inversion
ASD	Algorithm Specifications Document
ATBD	Algorithm Theoretical Basis Document
BESS	Breathing Earth Systems Simulator
DAAC	Distributed Active Archive Center
DisALEXI	ALEXI Disaggregation algorithm
ECOSTRESS	ECOsystem Spaceborne Thermal Radiometer on Space Station
ESI	Evaporative Stress Index
ET	Evapotranspiration
FLiES	Forest Light Environmental Simulator
GDS	Ground Data System
HDF	Hierarchical Data Format
Hz	Hertz

ICD	Interface Control Document
ISS	International Space Station
JPL	Jet Propulsion Laboratory
Km	kilometer
L0 – L4	Level 0 through Level 4
LP	Land Processes
LST	Land Surface Temperature
LSTE	Land Surface Temperature and Emissivity
m	meter
MODIS	Moderate Resolution Imaging Spectroradiometer
NASA	National Aeronautics and Space Administration
NCEP	National Centers for Environmental Protection
netCDF	Network Common Data Format
PCS	Process Control System
PGE	Product Generation Executable
PSD	Product Specifications Document
PT-JPL	Priestley-Taylor-JPL
QA	Quality Assurance
SDOS	Science Data Operations System
SDS	Science Data System
TBD	To Be Determined
TBR	To Be Reconciled
TBS	To Be Specified
USDA	United State Department of Agriculture
USGS	United States Geological Society
UTC	Coordinated Universal Time
WUE	Water Use Efficiency
XML	Extensible Markup Language

7.0 REFERENCES

Allen, R. G., M. Tasumi, and R. Trezza (2007), Satellite-based energy balance for mapping evapotranspiration with internalized calibration (METRIC)-model, *J. Irrig. Drain. E.*, *133*, 380-394.

Anderson, M. C., J. M. Norman, J. R. Mecikalski, J. A. Otkin, and W. P. Kustas (2007), A climatological study of evapotranspiration and moisture stress across the continental United States based on thermal remote sensing: 1. Model formulation, *J. Geophys. Res.*, *112*(D10), D10117.

Anderson, M. C., W. P. Kustas, C. R. Hain, C. Cammalleri, F. Gao, M. Yilmaz, I. Mladenova, J. Otkin, M. Schull, and R. Houborg (2013), Mapping surface fluxes and moisture conditions from field to global scales using ALEXI/DisALEXI, *Remote Sensing of Energy Fluxes and Soil Moisture Content*, 207-232.

Baldocchi, D. (2008), 'Breathing' of the terrestrial biosphere: lessons learned from a global network of carbon dioxide flux measurement systems, *Australian Journal of Botany, 56*, 1-26.

Baldocchi, D., E. Falge, L. H. Gu, R. J. Olson, D. Hollinger, S. W. Running, P. M. Anthoni, C. Bernhofer, K. Davis, R. Evans, J. Fuentes, A. Goldstein, G. Katul, B. E. Law, X. H. Lee, Y. Malhi, T. Meyers, W. Munger, W. Oechel, K. T. P. U, K. Pilegaard, H. P. Schmid, R. Valentini, S. Verma, T. Vesala, K. Wilson, and S. C. Wofsy (2001), FLUXNET: A new tool to study the temporal and spatial variability of ecosystem-scale carbon dioxide, water vapor, and energy flux densities, *Bulletin of the American Meteorological Society*, *82*(11), 2415-2434.

Bi, L., P. Yang, G. W. Kattawar, Y.-X. Hu, and B. A. Baum (2011), Diffraction and external reflection by dielectric faceted particles, *J. Quant. Spectrosc. Radiant. Transfer*, *112*, 163-173.

Bisht, G., V. Venturini, S. Islam, and L. Jiang (2005), Estimation of the net radiation using MODIS (Moderate Resolution Imaging Spectroradiometer), *Remote Sensing of Environment*, *97*, 52-67.

Bouchet, R. J. (1963), Evapotranspiration re´elle evapotranspiration potentielle, signification climatique*Rep. Publ. 62*, 134-142 pp, Int. Assoc. Sci. Hydrol., Berkeley, California.

Chen, X., H. Wei, P. Yang, and B. A. Baum (2011), An efficient method for computing atmospheric radiances in clear-sky and cloudy conditions, *J. Quant. Spectrosc. Radiant. Transfer*, *112*, 109-118.

Chen, Y., J. Xia, S. Liang, J. Feng, J. B. Fisher, X. Li, X. Li, S. Liu, Z. Ma, and A. Miyata (2014), Comparison of satellite-based evapotranspiration models over terrestrial ecosystems in China, *Remote Sensing of Environment*, *140*, 279-293.

Coll, C., Z. Wan, and J. M. Galve (2009), Temperature-based and radiance-based validations of the V5 MODIS land surface temperature product, *Journal of Geophysical Research*, *114*(D20102), doi:10.1029/2009JD012038.

Ershadi, A., M. F. McCabe, J. P. Evans, N. W. Chaney, and E. F. Wood (2014), Multi-site evaluation of terrestrial evaporation models using FLUXNET data, *Agricultural and Forest Meteorology*, *187*, 46-61.

Fisher, J. B., K. Tu, and D. D. Baldocchi (2008), Global estimates of the land-atmosphere water flux based on monthly AVHRR and ISLSCP-II data, validated at 16 FLUXNET sites, *Remote Sensing of Environment*, *112*(3), 901-919.

Fisher, J. B., R. H. Whittaker, and Y. Malhi (2011), ET Come Home: A critical evaluation of the use of evapotranspiration in geographical ecology, *Global Ecology and Biogeography*, *20*, 1-18.

Fisher, J. B., G. J. Moore, and M. K. Verma (2015), Net Radiation and Evapotranspiration (Rn/ET) Download Product Tools and Interfaces, in *NASA Tech Briefs*, edited, NASA.

Fisher, J. B., D. D. Baldocchi, L. Misson, T. E. Dawson, and A. H. Goldstein (2007), What the towers don't see at night: Nocturnal sap flow in trees and shrubs at two AmeriFlux sites in California, *Tree Physiology*, *27*(4), 597-610.

Fisher, J. B., S. Hook, R. Allen, M. Anderson, A. French, C. Hain, G. Hulley, and E. Wood (2014), The ECOsystem Spaceborne Thermal Radiometer Experiment on Space Station (ECOSTRESS): science motivation, paper presented at American Geophysical Union Fall Meeting, San Francisco.

Fisher, J. B., Y. Malhi, A. C. de Araújo, D. Bonal, M. Gamo, M. L. Goulden, T. Hirano, A. Huete, H. Kondo, T. Kumagai, H. W. Loescher, S. Miller, A. D. Nobre, Y. Nouvellon, S. F. Oberbauer, S. Panuthai, C. von Randow, H. R. da Rocha, O. Roupsard, S. Saleska, K. Tanaka, N. Tanaka, and K. P. Tu (2009), The land-atmosphere water flux in the tropics, *Global Change Biology*, *15*, 2694-2714.

García, M., I. Sandholt, P. Ceccato, M. Ridler, E. Mougin, L. Kergoat, L. Morillas, F. Timouk, R. Fensholt, and F. Domingo (2013), Actual evapotranspiration in drylands derived from in-situ and satellite data: Assessing biophysical constraints, *Remote Sensing of Environment*, *131*, 103-118.

Goulden, M. L., J. W. Munger, S. M. Fan, B. C. Daube, and S. C. Wofsy (1996), Measurements of carbon sequestration by long-term eddy covariance: methods and a critical evaluation of accuracy, *Global Change Biology*, *2*, 169-182.

Iqbal, M. (2012), *An introduction to solar radiation*, Elsevier.

Iwabuchi, H. (2006), Efficient Monte Carlo Methods for Radiative Transfer Modeling, *Journal of the Atmospheric Sciences*, *63*(9), 2324-2339.

June, T., J. R. Evans, and G. D. Farquhar (2004), A simple new equation for the reversible temperature dependence of photosynthetic electron transport: a study on soybean leaf, *Functional Plant Biology*, *31*(3), 275-283.

Jung, M., M. Reichstein, and A. Bondeau (2009), Towards global empirical upscaling of FLUXNET eddy covariance observations: validation of a model tree ensemble approach using a biosphere model, *Biogeosciences*, *6*, 2001-2013.

Kobayashi, H., and H. Iwabuchi (2008), A coupled 1-D atmosphere and 3-D canopy radiative transfer model for canopy reflectance, light environment, and photosynthesis simulation in a heterogeneous landscape, *Remote Sensing of Environment*, *112*(1), 173-185.

Lagouarde, J., and Y. Brunet (1993), A simple model for estimating the daily upward longwave surface radiation flux from NOAA-AVHRR data, *International Journal of Remote Sensing*, *14*(5), 907-925.

Liang, X., D. P. Lettenmaier, E. Wood, and S. J. Burges (1994), A simple hydrologically based model of land surface water and energy fluxes for general circulation models, *Journal of Geophysical Research*, *99*(D7), 14415-14428.

Mallick, K., A. Jarvis, J. B. Fisher, K. P. Tu, E. Boegh, and D. Niyogi (2013), Latent heat flux and canopy conductance based on Penman-Monteith, Priestley-Taylor equation, and Bouchet's complementary hypothesis, *Journal of Hydrometeorology*, *14*, 419-442.

Mallick, K., A. J. Jarvis, E. Boegh, J. B. Fisher, D. T. Drewry, K. P. Tu, S. J. Hook, G. Hulley, J. Ardö, and J. Beringer (2014), A Surface Temperature Initiated Closure (STIC) for surface energy balance fluxes, *Remote Sensing of Environment*, *141*, 243-261.

Miralles, D. G., T. R. H. Holmes, R. A. M. De Jeu, J. H. Gash, A. G. C. A. Meesters, and A. J. Dolman (2011), Global land-surface evaporation estimated from satellite-based observations, *Hydrol. Earth Syst. Sci.*, *15*(2), 453-469.

Monteith, J. L. (1965), Evaporation and the environment, *Symposium of the Society of Exploratory Biology*, *19*, 205-234.

Moore, G. (2015), Rn/ET Download Product Tools and Interfaces*Rep.*, Jet Propulsion Laboratory, California Institute of Technology, Pasadena.

Mu, Q., M. Zhao, and S. W. Running (2011), Improvements to a MODIS global terrestrial evapotranspiration algorithm, *Remote Sensing of Environment*, *111*, 519-536.

Papale, D., and A. Valentini (2003), A new assessment of European forests carbon exchange by eddy fluxes and artificial neural network spatialization, *Global Change Biology*, *9*, 525-535.

Penman, H. L. (1948), Natural evaporation from open water, bare soil and grass, *Proceedings of the Royal Society of London Series A*, *193*, 120-146.

Potter, C. S., J. T. Randerson, C. B. Field, P. A. Matson, P. M. Vitousek, H. A. Mooney, and S. A. Klooster (1993), Terrestrial ecosystem production: a process based model based on global satellite and surface data, *Global Biogeochemical Cycles*, *7*(4), 811-841.

Prata, A. J. (1996), A new long-wave formula for estimating downward clear-sky radiation at the surface, *Quarterly Journal of the Royal Meteorological Society*, *122*(533), 1127-1151.

Price, J. C. (1977), Thermal inertia mapping: a new view of the earth, *Journal of Geophysical Research*, *82*(18), 2582-2590.

Priestley, C. H. B., and R. J. Taylor (1972), On the assessment of surface heat flux and evaporation using large scale parameters, *Monthly Weather Review*, *100*, 81-92.

Roesch, A., C. Schaaf, and F. Gao (2004), Use of Moderate-Resolution Imaging Spectroradiometer bidirectional reflectance distribution function products to enhance simulated surface albedos, *Journal of Geophysical Research*, *109*(D12), doi: 10.1029/2004JD004552.

Ryu, Y., D. D. Baldocchi, H. Kobayashi, C. van Ingen, J. Li, T. A. Black, J. Beringer, E. van Gorsel, A. Knohl, B. E. Law, and O. Roupsard (2011), Integration of MODIS land and atmosphere products with a coupled-process model to estimate gross primary productivity and evapotranspiration from 1 km to global scales, *Global Biogeochem. Cycles*, *25*(4), GB4017.

Ryu, Y., D. D. Baldocchi, T. A. Black, M. Detto, B. E. Law, R. Leuning, A. Miyata, M. Reichstein, R. Vargas, C. Ammann, J. Beringer, L. B. Flanagan, L. Gu, L. B. Hutley, J. Kim, H. McCaughey, E. J. Moors, S. Rambal, and T. Vesala (2012), On the temporal upscaling of evapotranspiration from instantaneous remote sensing measurements to 8-day mean daily-sums, *Agricultural and Forest Meteorology*, *152*(0), 212-222.

Stone, P. H., S. Chow, and W. J. Quirr (1977), July climate and a comparison of January and July climates simulated by GISS general circulation model, *Monthly Weather Review*, *105*(2), 170-194.

Su, Z. (2002), The Surface Energy Balance System (SEBS) for estimation of turbulent heat fluxes, *Hydrology and Earth System Sciences*, *6*, 85-99.

Vinukollu, R. K., E. F. Wood, C. R. Ferguson, and J. B. Fisher (2011), Global estimates of evapotranspiration for climate studies using multi-sensor remote sensing data: Evaluation of three process-based approaches, *Remote Sensing of Environment*, *115*, 801-823.

Wang, K., P. Wang, Z. Li, M. Cribb, and M. Sparrow (2007), A simple method to estimate actual evapotranspiration from a combination of net radiation, vegetation index, and temperature, *Journal of Geophysical Research*, *112*(D15107), doi:10.1029/2006JD008351.

Wind, G., S. Platnick, M. D. King, P. A. Hubanks, M. J. Pavolonis, A. K. Heidinger, P. Yang, and B. A. Baum (2010), Multilayer cloud detection with the MODIS near-infrared water vapor absorption band, *Journal of Applied Meteorology and Climatology*, *49*, 2315-2333.

Yang, F., M. A. White, A. R. Michaelis, K. Ichii, H. Hashimoto, P. Votava, A.-X. Zhu, and R. R. Nemani (2006), Prediction of continental-scale evapotranspiration by combining MODIS and AmeriFlux data through support vector machine, *Geoscience and Remote Sensing, IEEE Transactions on*, *44*(11), 3452-3461.

Zhang, L., B. Wylie, T. Loveland, E. Fosnight, L. L. Tieszen, L. Ji, and T. Gilmanov (2007), Evaluation and comparison of gross primary production estimates for the Northern Great Plains grasslands, *Remote Sensing of Environment*, *106*(2), 173-189.

Zhang, Q., X. Xiao, B. H. Braswell, E. Linder, J. Aber, and B. Moore (2005), Estimating seasonal dynamics of biophysical and biochemical parameters in a deciduous forest using MODIS data and a radiative transfer model, *Remote Sensing of Environment*, *99*, 357-371.